Journal of Nuclear Materials 392 (2009) 568–577

Contents lists available at ScienceDirect

Journal of Nuclear Materials

journal homepage: www.elsevier.com/locate/jnucmat

Review

Thermophysical properties of solid and liquid pure and alloyed Pu: A review

M. Boivineau *

CEA, Centre de Valduc, Département de Recherches sur les Matériaux Nucléaires, F-21120 Is-sur-Tille, France

ARTICLE INFO

Article history:
Received 11 June 2008
Accepted 9 April 2009

ABSTRACT

The thermophysical properties of both solid and liquid pure and alloyed plutonium have been investigated up to 4000 K by use of a resistive pulse heating technique, the so-called isobaric expansion experiment (IEX). Electrical resistivity, specific volume (density), latent heats of transformations, heat of fusion have been measured and extended in the whole liquid region. Additional static measurements have been also performed in order to determine the heat transport properties such as heat capacity, thermal diffusivity and thermal conductivity of plutonium alloys. After a first part devoted to additional results on pure Pu under rapid heating, this paper mostly deals with studies on different δ-stabilized Pu alloys in the high temperature range, particularly in the liquid state which is the principal originality of this work. In addition to the thermophysical data mentioned above, an attention is also paid onto sound velocity measurements on these alloys in the solid and liquid states. Hence, an anomalous behavior such as elastic softening is confirmed in the δ phase as already reported previously. Moreover, sound velocity and equation of state parameters (adiabatic and thermal bulk moduli, Grüneisen parameter, and specific heats ratio) have been investigated on liquid alloyed Pu. Such results confirm previous works on liquid pure Pu by presenting an atypical dual behavior of sound velocity, and are discussed in terms of delocalization process of the 5f electrons of both liquid pure and alloyed Pu.

Contents

1. Introduction

The physical properties of both pure and alloyed plutonium have been investigated under rapid heating by use of the Isobaric Expansion Experiment (IEX) described elsewhere in [1,2]. Such a device has been shown to be relevant for studying thermophysical properties and for providing numerous data in both the solid and liquid states of metals [3], this latter being the main originality of this work.

Most of the experiments on pure plutonium under rapid heating have been already published [2]. We report here additional data regarding the effect of heating rate on phase transformations in order to propose a dynamic pressure–temperature phases diagram under low pressure ($P < 0.4$ GPa).

The main novelty of this work concerns δ-stabilized Pu alloys. Indeed, it is known that the delta phase of pure plutonium (face-centered cubic), which is stable between 592 and 724 K, can be retained at room temperature by alloying plutonium with delta

* Corresponding author. Tel.: +33 3 80 23 41 62; fax: +33 3 80 23 52 17.
E-mail address: michel.boivineau@cea.fr.

0022-3115/$ - see front matter © 2009 Elsevier B.V. All rights reserved.
doi:10.1016/j.jnucmat.2009.04.008

phase stabilizer elements (so-called deltagens), such as gallium, aluminum, americium, cerium [4]. Delta stabilized plutonium alloys are solid solutions where the solute atoms substitute to plutonium atoms in the cubic lattice.

By alloying Pu, the number of allotropic phases versus temperature (at ambient pressure) is reduced from six for pure Pu down to two phases for alloyed Pu, the remaining phases being the δ (fcc) and ε (bcc). We have then investigated thermophysical properties of solid and liquid states of such alloys of different compositions of deltagen elements under both static and rapid heating conditions.

2. Experimental

2.1. General considerations

The Isobaric Expansion Experiment (IEX) consists in resistively heating (by Joule effect) metallic wires (typically 1 mm diameter, 30 mm length) by discharging a 60-kJ capacitor bank (20 kV, 30 kA, 300 μF) in about 100 μs [1,2]. Consecutive heating rates of 10^6–10^8 K · s^{-1} are produced, and significantly reduce the thermal and radiative losses, while sample remaining in the *thermodynamical equilibrium*. The sample takes place in an argon gas-filled pressure vessel (up to 0.6 GPa), and then operates in containerless conditions by avoiding contamination with its environment due to the sample reactivity [3]. Most of experiments have been conducted under a 0.12 GPa pressure.

2.2. Basic measurements and calculated parameters

At any period of time, the following measurements are available: (i) current intensity through the sample $I(t)$; (ii) voltage drop across the sample $U(t)$; (iii) diameter of the sample $\phi(t)$; and (iv) thermal emission from the heated sample $J(t)$. The current intensity, voltage, and diameter are measured with an uncertainty of ±0.6%, ±0.6% and ±1%, respectively.

From these measured quantities, thermophysical parameters, namely, enthalpy H(t), electrical resistivitiy $\rho_{el}(t)$, specific volume $V(t)/V_0$ (and consequently density variation $\rho(t)/\rho_0$), and temperature $T(t)$ are calculated. By combining these different terms (where t is time), one obtains $H(T)$, $\rho_0(T)$, $\rho_0(H)$, $\rho(T)$, $\rho(H)$, $V/V_0(T)$, $V/V_0(H)$, and the specific heat at constant pressure C_p. Electrical resistivity, specific volume and enthalpy are measured with an uncertainties of ±4%, ±5% and ±2%, respectively.

Sound velocity measurements, and deduced equation of state parameters (isothermal and adiabatic bulk moduli, isothermal and adiabatic compressibilities, Grüneisen parameter, specific heat ratio) can be also obtained with such a technique, whose principle and details are given elsewhere in [2,3].

3. Results and discussion

3.1. Complements on pure Pu

In addition to previous works devoted to the thermophysical properties of pure Pu [2], the effect of the *heating rate* has been investigated by studying the temperature evolution for different transitions, and for determining the *P–T phase diagram* under *rapid heating* conditions compared to static measurements. 99.95% purity electrorefined Pu samples have been studied. Their typical chemical composition is given in Table 1.

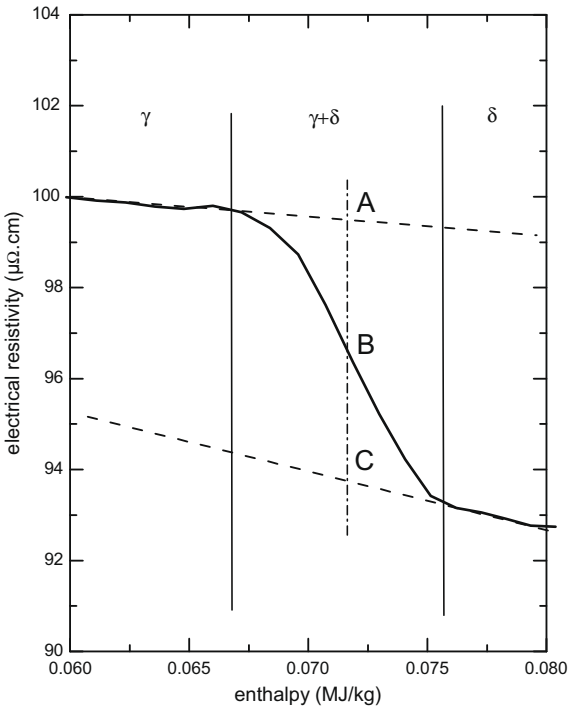

Fig. 1. Procedure for determining the transformation rate τ. The example is given for γ–δ.

It should be first pointed out that all the solid–solid transformations temperatures under rapid heating present higher values than for static ones. Such a phenomenon is not surprising since a similar effect of heating rate has been already exhibited for alloys such as TA6V [5]. Moreover, *the enthalpy of melting is independent on heating rate*: indeed, whatever the heating rate, the 130 kJ · kg^{-1} enthalpy value for reaching the liquid phase is always the same [2].

The transformation rate has been studied in the $8 \cdot 10^6$–6.10^7 K · s^{-1} (by changing the energy bank voltage) for the whole transitions in Pu. In order to determine such a rate without any temperature measurement in the solid state (the optical pyrometers start working at around 1800 K) we have analyzed the electrical resistivity variation as a function of enthalpy. The γ–δ transition is used here as an example and is shown in Fig. 1.

During the transition, when both phases A and B are present together, the electrical resistivity is supposed to go towards from the initial phase (A) to the final state one (B). After having linearly extrapolated the electrical resistivity variation of each phase, the transformation rate τ (*i.e.* the percentage of created phase B) is then calculated as follows (see Fig. 1):

$$\tau \cdot 100 = \frac{AB}{AC}, \quad (1)$$

where $0 < \tau < 1$.

Table 1
Typical chemical compositions (in wt ppm) of electrorefined plutonium samples.

Element	Al	^{241}Am	Cr	Cu	Fe	Ga	Ni	Ta	Pu
Composition (wt ppm)	20	10	5	10	15	20	20	100	balance

Table 2
Transition enthalpies values in $kJ \cdot kg^{-1}$ for solid Pu.

Transition	Ref. [6]	Ref. [7]	Working data
$\alpha \rightarrow \beta$	14.66	15.5	15
$\beta \rightarrow \gamma$	2.03	2	2.015
$\gamma \rightarrow \delta$	2.74	2.98	2.86
$\delta' \rightarrow \varepsilon$	6.76		6.76

Table 3
Averaged heat capacities (in $J \cdot kg^{-1} \cdot K^{-1}$) of the different Pu solid phases used in this work [6,7].

Phase	C_p ($J \cdot kg^{-1} \cdot K^{-1}$)
α	141 ± 1.3
β	139 ± 1
γ	144 ± 1.3
δ, δ'	149 ± 4.5
ε	141 ± 7

Different assumptions are given as follows:

- during the transition, the electrical resistivity is proportional to the volume percentage of both phases, and is a linear function of the deposited energy,
- the A → B transition enthalpy is proportional to the transformation rate,
- as long as the transition A → B is operating, an energy quantity $\tau \cdot \Delta H_T$ (ΔH_T being the literature recommended value for the transition enthalpy) is used. If the enthalpy experimental value between the start and the end of the transition ΔH_{AB}, is found to be higher than ΔH_T, then the additional energy is considered to be as a temperature elevation[1],
- we have used different physical constants reported in literature [6,7] and summarized in Table 2. The working data correspond to an average of both data.

In order to determine the temperature, we have used averaged values of heat capacities at constant pressure of each phase as shown in Table 3 [6,7]. With such values and assumptions, we have then calculated *the temperature increase during the transformation* as presented in Fig. 2 for the α–β case. It should be noticed that this curve is independent on heating rate (in the studied region), which is not the case for other transitions. One should also mention that the α–β transition operates at constant temperature up to a 40% transformation rate and continues with a temperature increase at higher rates.

The effect of *heating rate* has been also studied, and is reported in Fig. 3 for the γ–δ transition. A linear fit of experimental data is found to be:

$$\Delta T(K) = 0.9 \cdot 10^{-6} \cdot a, \quad (2)$$

where a is the heating rate (in $K \cdot s^{-1}$).

It should be pointed out that, since this curve crosses the zero point, it means this transition operates under isothermal conditions at very low heating rates. Moreover, the transition start temperatures do not depend on the heating rate.

By combining both the literature data of Tables 2 and 3 and our own data, we have been then able to obtain the *P–T* phase diagram at low pressure ($P \leqslant 0.2$ GPa for pressures at P_{amb}, 0.05, 0.11, 0.124, and 0.2 GPa) under *rapid heating conditions*.

[1] This elevation is calculated as follows: $\Delta T = C_p \cdot (\Delta H_{AB} - \Delta H_T)$.

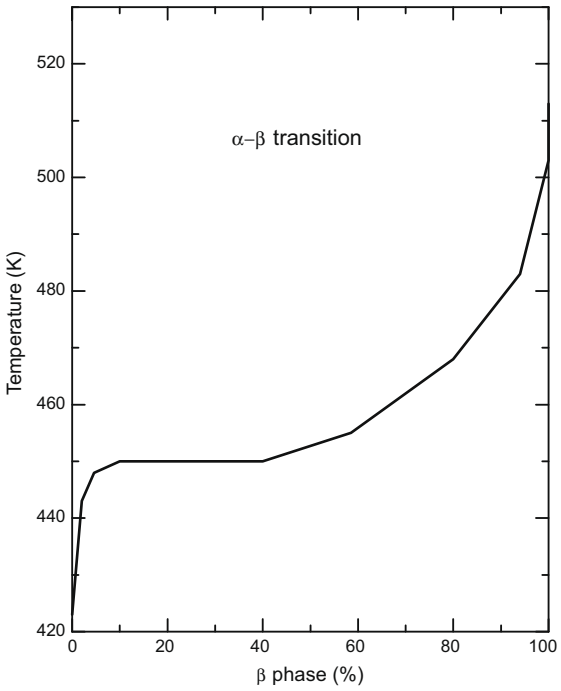

Fig. 2. Temperature variation during the α–β transition.

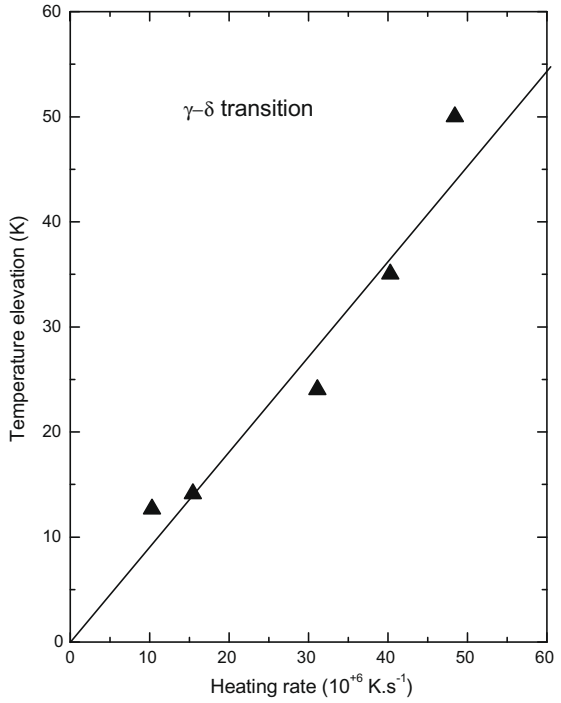

Fig. 3. Temperature increase versus heating rate during the γ–δ transformation.

Such a diagram is reported in Fig. 4, as for literature data [8,9].

The comments on this diagram lead to first conclusions:

- the α–β transition temperature is 46 K higher than static data (378 K at P_{amb}), and its slope of 117 $K \cdot GPa^{-1}$ is in excellent agreement with the 112 $K \cdot GPa^{-1}$ value obtained by Stephens [8],
- the β–γ transition is not well precisely established in rapid heating conditions,

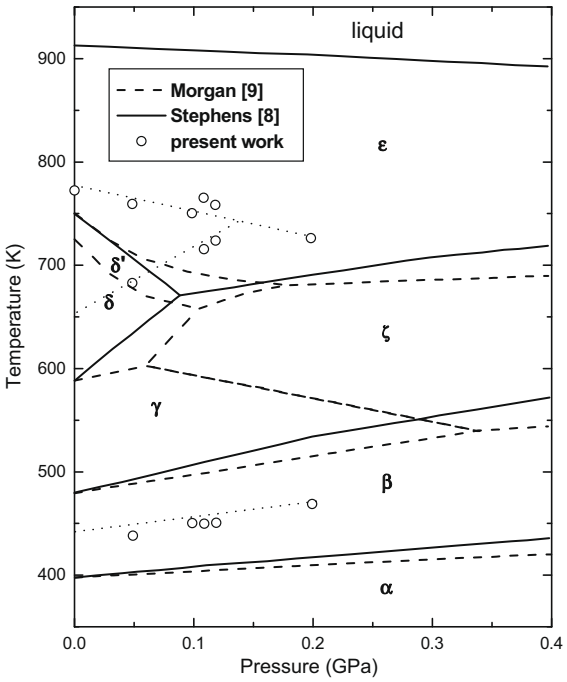

Fig. 4. Dynamic low pressure *P–T* phase diagram of pure Pu.

- the γ–δ transition occurs at 658 K at P_{amb}, 70 K higher than the static data (588 K). Its evolution is close to Stephen's one [8],
- due to its very low electrical resistivity variation, the δ–δ′ is only observed at ambient pressure [2],
- the δ'–ε is 20 K higher, when comparing with static data. Its evolution is similar to Morgan's curve [9],
- the γ, δ, ε *triple point* was found to be at 738 K and 0.147 GPa.

To summarize this section devoted to additional physical properties of pure Pu under *rapid heating conditions*, and the determination of the dynamic *P–T* phase diagram at low pressure ($P \leqslant 0.2$ GPa) of *unalloyed Pu*, one can conclude that in unalloyed Pu, during rapid heating:

- the allotropic transition temperatures are systematically and significantly higher than the static measurements,
- the transition start temperatures do not depend on the heating rate,
- the needed deposited enthalpy value for reaching the liquid state (130 $kJ \cdot kg^{-1}$), and consequently the melting point, is the same as static data, and is *independent* on the heating rate,
- the 11.6 $kJ \cdot kg^{-1}$ heat of fusion [2] is in excellent agreement with the 11.75 $kJ \cdot kg^{-1}$ recommended static value [7].

3.2. Studies of alloys

Different compositions of δ-stabilized plutonium alloys have been investigated, gallium being the main solute. The typical deltagen elements composition of such δ-Pu alloys is given in Table 4. Four different deltagens contents have been investigated: 1.5, 2.5, 3.6 and 6.1 at.%. All of these alloys have undergone a 200 h heat treatment duration at 733 K in order to get homogenized samples.

An additional 0.4 at.% deltagen composition alloy (indicated as α-Pu 0.4 at.%) has been also studied. It should be noticed that, according to PuGa phases diagram [10] such an alloy differs from the others. Since it is not δ single phased but is stabilized in the α+δ phase.

Table 4
Typical deltagen elements chemical compositions (in at.%) of studied plutonium alloys.

Deltagen element	Al	Am[a]	Ga
Pu alloy			
α-Pu 0.4 at.%	0.05	0.1	0.25
δ-Pu 1.5 at.%	0.06	0.13	1.28
δ-Pu 2.5 at.%	0.1	0.2	2.2
δ-Pu 3.6 at.%	0.09	0.21	3.28
δ-Pu 6.1 at.%	0.02	0.03	6

[a] Content value measured at the present study.

3.2.1. The solid state

3.2.1.1. Heat transport properties. Classical static experimental devices have been used to investigate the heat transport properties of delta domain and phase transformations for different Pu alloys. For instance, the *heat capacity* of such alloys has been determined using a Differential Scanning Calorimeter (Setaram DSC 111). Such results are presented in Fig. 5 in the 300–1000 K temperature range, the uncertainty being ±6%. Fig. 5 clearly indicates that both the δ–ε and ε-liquid transitions occur at 825 and 950 K, respectively for the δ-Pu 2.5 at.% alloy.

Other heat capacity measurements of δ-Pu alloys have also been investigated in the only δ phase domain, and are reported in Fig. 5. Comparison with literature data of similar deltagen element compositions [11,12] shows a good agreement even if our values are slightly lower. Moreover an increase of data dispersion at high temperature (from ~700 K) is observed. In all cases, the δ phase heat capacity is found to increase with temperature.

Additional data on pure α-Pu and α-Pu 0.4 at.% are also reported from room temperature to the α–β transformation temperature (~393 K). Such results indicate higher values than those of δ-Pu alloys and show that their heat capacity is constant versus temperature.

The best polynomial fits of the different alloys are summarized in Table 5.

Thermal diffusivity of Pu alloys has been also investigated. An equipment enclosed in a glove box has been specially designed to implement the 'laser flash' technique for studying actinides. The front surface of a disk-shaped specimen (high-frequency induction is used to heat the sample in 2 mbar nitrogen atmosphere) was heated instantaneously with use of a ~30 J/1 ms pulse Nd-glass laser. The temperature rise on the back face was measured using a chromel–alumel thermocouple wires contacting the Pu samples. The rear surface temperature was monitored on

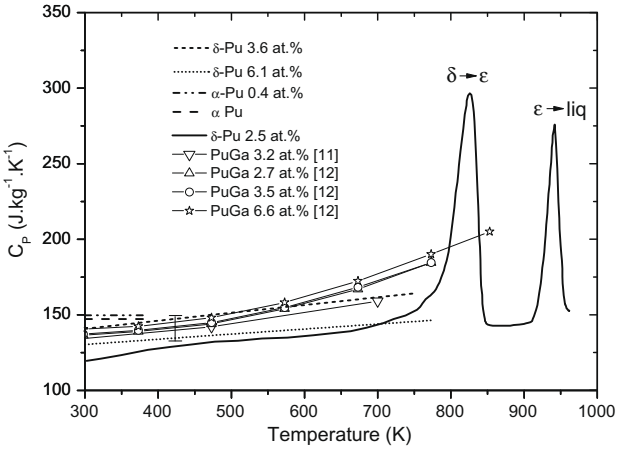

Fig. 5. Heat capacity versus temperature for different Pu alloys compared with literature data [11,12].

Table 5
Best polynomial fits of heat capacity C_p, thermal diffusivity a and thermal conductivity λ of Pu alloys versus temperature (in K) and comparison with available literature data [11–13].

Alloy	C_p ($J \cdot kg^{-1} \cdot K^{-1}$)	a ($cm^2 \cdot s^{-1}$)	λ ($W \cdot m^{-1} \cdot K^{-1}$)
α-Pu[a]	147.3	$a \times 10^2 = 1.28 + 2.37 \cdot 10^{-3}\ T$	$\lambda = 3.7 + 6.84 \cdot 10^{-3}\ T$
α-Pu 0.4 at.% [a]	149.8	$a \times 10^2 = 1.1 + 3.74 \cdot 10^{-3}\ T$	$\lambda = 3.08 + 1.06 \cdot 10^{-2}\ T$
δ-Pu 2.5 at.%	$106 + 5.4 \cdot 10^{-2}\ T$	$a \times 10^2 = 1.474 + 7.6 \cdot 10^{-3}\ T$	$\lambda = 2.64 + 1.3 \cdot 10^{-2}\ T + 7.3 \cdot 10^{-6}\ T^2$
δ-Pu 3.6 at.%	$126 + 5.11 \cdot 10^{-2}\ T$	$a \times 10^2 = 2.23 + 5.85 \cdot 10^{-3}\ T$	$\lambda = 4.4 + 1.33 \cdot 10^{-2}\ T + 4.7 \cdot 10^{-6}\ T^2$
δ-Pu 6.1 at.%	$120{,}5 + 3.34 \cdot 10^{-2}\ T$	$a \times 10^2 = 0.13 + 1.44 \cdot 10^{-2}\ T + 7.54 \cdot 10^{-6}\ T^2$	$\lambda = 0.174 + 2.83 \cdot 10^{-2}\ T + 9.9 \cdot 10^{-6}\ T^2$
PuGa 3.2 at.%[b]	$115 + 6.2 \cdot 10^{-2}\ T$		
PuGa 2.7 at.%[c]	$150.6 - 10^{-1}\ T + 1.9 \cdot 10^{-4}\ T^2$	$a \times 10^2 = 1.86 + 7.1 \cdot 10^{-3}\ T$	$\lambda = 7.16 - 3.54 \cdot 10^{-3}\ T + 2.8 \cdot 10^{-5}\ T^2$
PuGa 3.5 at.% [c]	$149.2 - 9.4 \cdot 10^{-2}\ T + 1.8\ 10^{-4}\ T^2$	$a \times 10^2 = 1.69 + 7.0 \cdot 10^{-3}\ T$	$\lambda = 6.9 - 3.84 \cdot 10^{-3}\ T + 2.8 \cdot 10^{-5}\ T^2$
PuGa 6.6 at.%)[c]	$152 - 9.45 \cdot 10^{-2}\ T + 1.85\ 10^{-4}\ T^2$	$a \times 10^2 = 1.33 + 6.9 \cdot 10^{-3}\ T$	$\lambda = 6.32 - 4.2 \cdot 10^{-3}\ T + 2.76 \cdot 10^{-5}\ T^2$
PuGa 1 wt%[d]		$a \times 10^2 = 1.89 + 6.08 \cdot 10^{-3}\ T$	

[a] For 300 K < T < $T_{\alpha-\beta}$ (~393 K).
[b] Ref. [11].
[c] Ref. [12].
[d] Ref. [13].

a numerical oscilloscope. Thermal diffusivity is then automatically calculated with a microcomputer. The uncertainty is found to be ±7%.

Results are presented in Fig. 6 and compared with literature data [12,13], and mainly concern the δ phase temperature domain, except for the δ-Pu 2.5 at.% alloys which includes the δ–ε transition. It is shown that thermal diffusivity increases as a function of temperature in all cases. Here again, comparison with literature data [12,13] indicates a good agreement. Moreover, pure α-Pu and α-Pu 0.4 at.% show lower values than for δ-Pu alloys, and slightly increase with temperature.

The best polynomial fits are gathered in Table 5 as those of literature data.

From heat capacity C_p and thermal diffusivity a, *thermal conductivity* λ can be calculated according to:

$$\lambda = a \cdot \rho \cdot C_p, \tag{3}$$

where ρ is density, the working data (assumed to be constant values) being $18.9 \cdot 10^3\ kg \cdot m^{-3}$ for the α-Pu 0.4 at.% alloy and 15.8, 15.75, $15.66 \cdot 10^3\ kg \cdot m^{-3}$ for our δ-Pu 2.5, 3.6 and 6.1 at.% alloys, respectively. The uncertainty of thermal conductivity is ±15%.

Here again, thermal conductivity increases with temperature as shown in Fig. 7 and even if a dispersion of data is observed at high temperature (from ~700 K), a good agreement is observed with literature data [12]. Moreover, thermal conductivities of α-Pu and α-Pu 0.4 at.% are significantly lower than for the δ-Pu alloys. The best polynomial fits are gathered in Table 5.

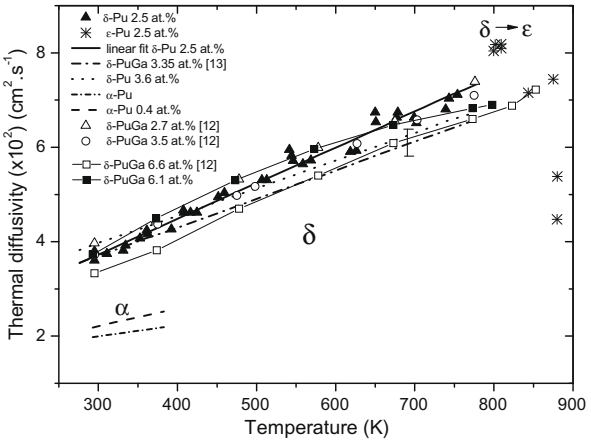

Fig. 6. Thermal diffusivity versus temperature for different Pu alloys compared with literature data [12,13].

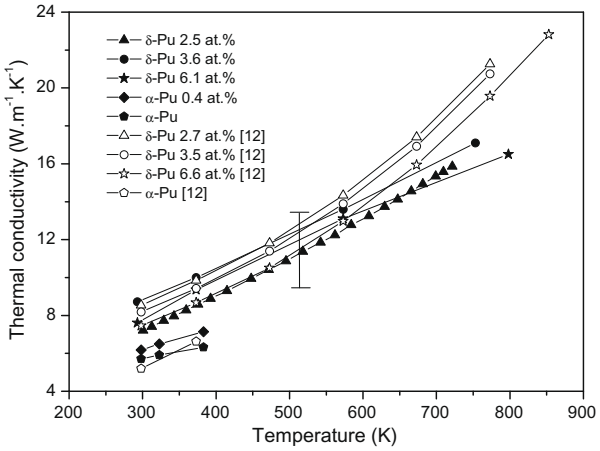

Fig. 7. Thermal conductivity versus temperature for different Pu alloys compared with literature data [12].

From a general point of view, one can remark that the deltagen elements composition has not a strong influence on these heat transport properties.

3.2.1.2. Electrical resistivity. The electrical resistivity has been studied for different δ-Pu alloys: 2.5, 3.6 and 6.1 at.%. A compilation is shown in Fig. 8 versus enthalpy (temperature measurements being not possible with optical pyrometry in this low temperature range). All of the curves clearly indicate the δ–ε transformation and melting from the observation of electrical resistivity variations.

Moreover, it should be noticed that heating rate leads to an elevation of around 50 K for the δ–ε transformation. On the other hand, no effect of rapid heating is observed for melting (as for pure Pu).

From these curves it is possible to determine the *heats of transformation* (see Section 3.2.1.3), including melting. For lightening Fig. 8, the way of determining phase domains is only shown for the example of δ-Pu 3.6 at.% alloy (see vertical dotted lines).

3.2.1.3. Heats of transformations. Phase transformations enthalpies data have been investigated from previous results using either static data (e.g.: DSC) or rapid heating measurements with the isobaric expansion experiment with use of electrical resistivity. Such results are presented in Table 6 for three different δ-Pu alloys: 2.5, 3.6 and 6.1 at.%. Then it can be seen that the latent heat values under rapid heating are systematically and significantly higher

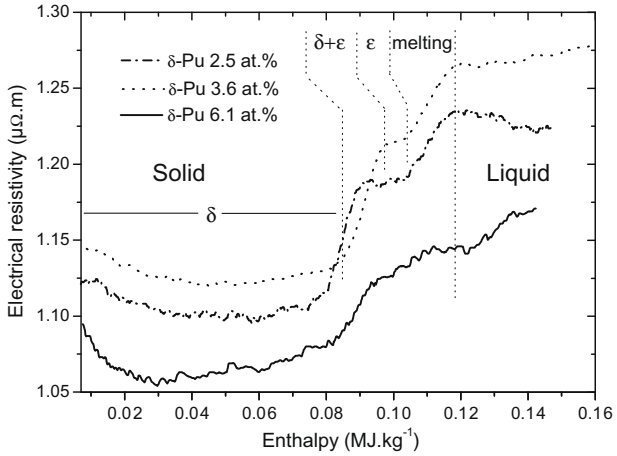

Fig. 8. Electrical resistivity versus enthalpy of solid δ-Pu 2.5, 3.6 and 6.1 at.% alloys up to melting.

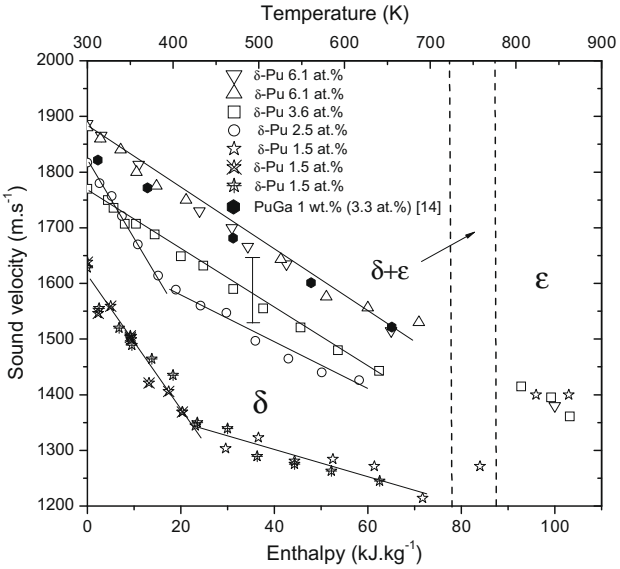

Fig. 9. Longitudinal sound velocity versus enthalpy (temperature) of solid δ-Pu 1.5, 2.5, 3.6 and 6.1 at.% alloys.

Table 6
Enthalpies of δ–ε transformation and melting of the studied δ-Pu alloys under static and rapid heating conditions.

Alloy	$\Delta H_{\delta-\varepsilon}$ (kJ · kg^{-1})	ΔH_{melt} (kJ · kg^{-1})
δ-Pu 2.5 at.%[a]	12.9 ± 0.5	14.9 ± 0.5
δ-Pu 3.6 at.%	7.52 ± 0.4	11.7 ± 1.2
δ-Pu 3.6 at.% [a]	11.1 ± 0.5	12.7 ± 0.5
δ-Pu 6.1 at.%	7.52 ± 0.4	11.5 ± 1.2
δ-Pu 6.1 at.% [a]	11.9 ± 0.5	14 ± 0.5
Pure Pu[a] [2]	15.3 ± 0.5	11.6 ± 0.5

[a] Under rapid heating.

than those obtained in static conditions. Such a phenomenon has been already observed for pure Pu as reported in Section 3.1.

Moreover, it should be noticed that the needed enthalpy value for reaching the liquid state is 120 kJ·kg^{-1} (130 kJ·kg^{-1} for pure Pu) for these alloys (see Fig. 8), and is *independent* on the heating rate.

3.2.1.4. Sound velocity. Sound velocity measurements which have been detailed elsewhere [2,3], have been investigated for 1.5, 2.5, 3.6 and 6.1 at.% δ-Pu alloys in the solid phase. Briefly, the principle consists in launching a laser-generated stress wave in the sample by focusing the output of a pulsed laser onto one side of the sample. The resulting instantaneous stress wave, which is spherically diverging and degrading into an acoustic wave, propagates through the sample and emerges on the side opposite the laser source. A streak camera record gives the transit time of the acoustic wave propagating through the sample diameter. Sound velocity is deduced when knowing the diameter value (which is measured from radial expansion). Typically, uncertainty is found to be around ±5%. One has to mention the longitudinal component is only reachable throughout such a device.

Longitudinal sound velocity measurements of different δ-Pu alloys are presented in Fig. 9. These results indicate a linear decrease versus enthalpy (temperature) for higher deltagens contents (3.6 and 6.1 at.%) as shown from linear fits used as guidelines. Such a linear behavior was already observed by Calder et al. [14] for the delta-stabilized PuGa 1 wt% (∼3.3 at.%) alloy, whose values are reported in Fig. 9 for comparison. When comparing these sound velocity values to our closest δ-Pu 3.6 at.% alloy, one can remark that our data are around 80 m·s^{-1} lower, which means around 4.5% lower (and then included in the error bars), the slopes being very similar.

On the other hand a *inflexion point* is observed for lower contents such as 1.5 and 2.5 at.% (see guidelines on Fig. 9). A similar phenomenon has been already observed by Migliori et al. [15] for the PuGa 2.4 at% using resonant ultrasound spectroscopy (RUS) by reporting a jog of the shear modulus and bulk modulus versus temperature. In this paper, the authors mentioned an unexpected *elastic softening* in δ-Pu with increasing temperature despite negligible thermal expansion, later on interpreted by using a so-called two-level 'Invar'-like model by Lawson et al. [16]. Such a model accounts satisfactorily for interpreting the anomalous thermodynamic properties of the δ-phase of pure and alloyed Pu, by introducing two additional parameters which both depend strongly on Ga composition: the energy spacing ΔE (∼1400 K·atom^{-1}) of a hypothetical Invar excited state and the electronic Grüneisen parameter Γ which is found to be negative. This model accounts for the anomalous decrease in the bulk modulus with temperature by assuming a zero elastic stiffness for the excited electronic state.

One has to mention that the inflexion point at around 400 K for our δ-Pu 2.5 at.% alloy occurs at the same temperature of the jog of bulk modulus and shear modulus observed by Migliori et al. [15] for the PuGa 2.4 at%. A similar behavior is observed at around 430 K for the δ-Pu 1.5 at.% alloy (see Fig. 9). Since such a phenomenon is not observed for higher contents it could be correlated to the *metastability* region of the δ phase for low solute contents (when [Ga] < 3 at.%), associated with the existence of a martensitic transformation occurring at low temperature [4].

On the opposite, composition has a small effect on sound velocity of the ε phase since it is equal to around 1400 m·s^{-1} for the whole alloys.

3.2.2. The liquid state

As mentioned before, we have investigated and focused our attention on the liquid state. Only a few reported data have been obtained in liquid, and in any case, for a low temperature range. We report here a much higher temperature range (up to around 4000 K) which then corresponds to the main novelty of this work.

3.2.2.1. Thermophysical data. As for solid state, electrical resistivity and specific volume variation have been determined in the liquid domain using specifically the isobaric expansion experiment. A

compilation of the electrical resistivity of liquid δ-Pu 2.5 and 6.1 at.% alloys is presented in Fig. 10. Drastic changes of resistivity correspond to phase transformations including melting. One can then clearly distinguish the solid and liquid phases as it is shown for the δ-Pu 2.5 at.% alloy (see vertical lines and corresponding transformations). The maximum deposited enthalpy value of 800 kJ·kg^{-1} obtained for the δ-Pu 6.1 at.% alloy corresponds to around 4200 K (by extrapolating the $\Delta H = f(T)$ curve of Fig. 12).

Specific volumes measurements are also presented in Fig. 11, and are reported as a function of enthalpy for liquid δ-Pu 3.6 and 6.1 at.%. As for electrical resistivity, volume changes associated to phase transformations are clearly displayed. For lightening Fig. 11, the phase stability domains are only shown for the δ-Pu 3.6 at.% alloy.

The study of the liquid state at elevated temperature ($T > 1800$ K) is compatible with use of multispectral pyrometry by assuming emissivity to be independent on temperature and wavelength, but leading to a high uncertainty (±10%) of temperature measurements.

Then, liquid δ-Pu 6.1 at.% volume variation is presented versus temperature in Fig. 12. From this curve, one can deduce the volume thermal expansion coefficient α defined as:

$$\alpha = \frac{1}{V}\left(\frac{\partial V}{\partial T}\right)_P. \tag{4}$$

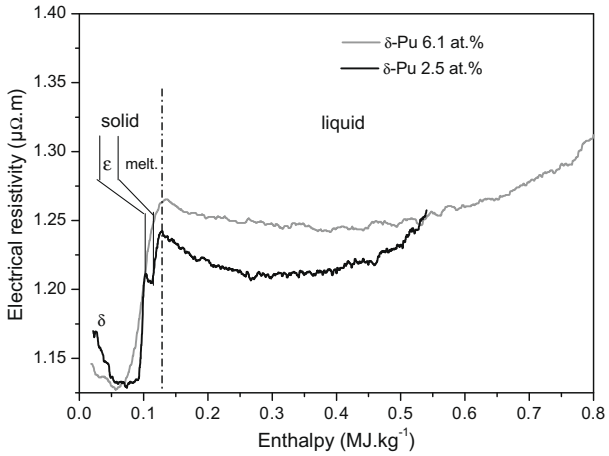

Fig. 10. Electrical resistivity versus enthalpy of solid and liquid δ-Pu 2.5 and 6.1 at.% alloys.

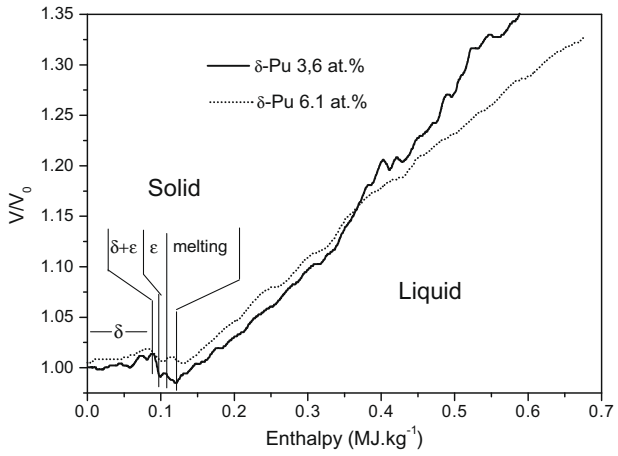

Fig. 11. Specific volume versus enthalpy of solid and liquid δ-Pu 3.6 and 6.1 at.% alloys.

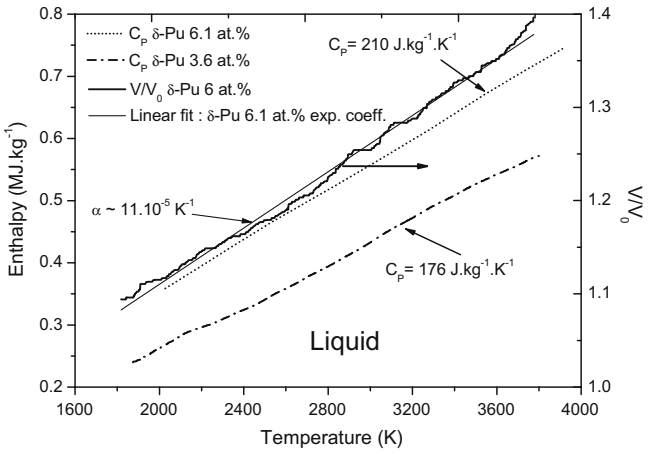

Fig. 12. Enthalpy of liquid δ-Pu 3.6 and 6.1 at.% alloy versus temperature, and specific volume versus temperature of liquid δ-Pu 6.1 at.% versus temperature.

The best linear fit of this curve gives a $11{\cdot}10^{-5}$ K^{-1} value, same one as pure Pu [2], meaning that this low solute content has a negligible influence.

The enthalpy variation is also reported as a function of temperature for liquid δ-Pu 3.6 and 6.1 at.% in Fig. 12. The slopes of such curves correspond to the heat capacity since:

$$C_p = \left[\frac{\partial H(T)}{\partial T}\right]_{P=cst}, \tag{5}$$

Then liquid δ-Pu 3.6 and 6.1 at.% heat capacity values are found to be 176 and 210 J·kg^{-1}·K^{-1}, respectively, with an uncertainty of ±15%. One can notice the reported pure liquid plutonium value is 177 J·kg^{-1}·K^{-1} in the low temperature range [6,7].

3.2.2.2. Sound velocity. Sound velocity measurements have been developed on pulse heating devices to provide equation of state (EOS) parameters of liquid metals [2,3,17].

Since the shear component is negligible in the liquid, sound velocity of liquid c_l is defined as:

$$C_l = c_L, \tag{6}$$

where c_L is the longitudinal component of the sound velocity in the liquid phase. For convenience, one introduces the adiabatic B_S and isothermal B_T bulk moduli, inversely equal to their corresponding compressibility χ_S and χ_T, and defined as follows:

$$B_S = \frac{1}{\chi_S} = -V\left(\frac{\partial P}{\partial V}\right)_{S=cst} = \rho\left(\frac{\partial P}{\partial \rho}\right)_{S=cst} = \rho c_L^2, \tag{7}$$

where ρ is density. χ_S, χ_T, B_S, and B_T are related by the following expression:

$$\frac{B_S}{B_T} = \frac{\chi_T}{\chi_S} = \gamma, \tag{8}$$

where γ is the specific heat ratio also expressed by:

$$\gamma = \frac{C_p}{C_v} = 1 + T\alpha\Gamma, \tag{9}$$

where C_p and C_v are the specific heats at constant pressure and constant volume, respectively, T is the absolute temperature (in K) and α is the volume thermal expansion coefficient (see Eq. (4)). In Eq. (9), Γ is the Grüneisen parameter (which links pressure on the sample to its internal energy) commonly used and expressed by:

$$\Gamma = V\left(\frac{\partial P}{\partial E}\right)_V = \alpha\frac{c_L^2}{C_p}. \tag{10}$$

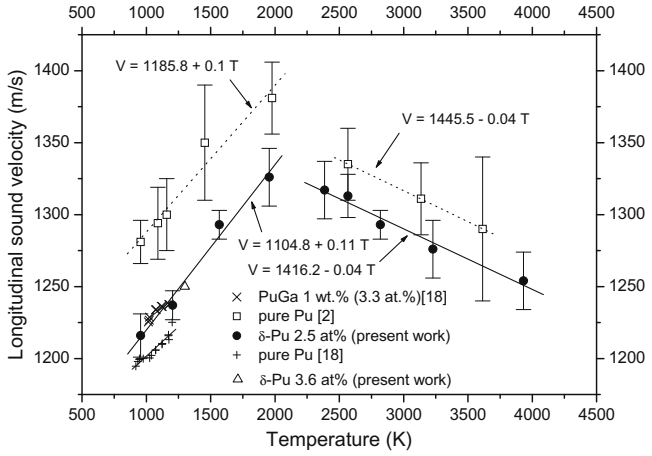

Fig. 13. Longitudinal sound velocity versus temperature of liquid δ-Pu 2.5 at.% alloy and liquid pure Pu [2], and comparison with literature data [18].

These equations show the utility and convenience of sound velocity for determining the EOS parameters particularly in the liquid (no shear component).

Results of longitudinal sound velocity on liquid 2.5, 3.6 (1 point) at.% δ-Pu alloys and pure Pu [2] are reported versus temperature in Fig. 13. Our results are compared with the only available literature data reported in a much lower temperature range obtained on pure Pu and PuGa 1 wt% alloy by Merz et al. [18].

It can be seen strong similarities of liquid pure and alloyed Pu. Indeed, as for pure Pu a maximum of sound velocity is observed at around 2000 K for the δ-Pu 2.5 at.% alloy. Moreover, the alloying effect tends to lower sound velocity of 60 $m{\cdot}s^{-1}$ from melting to 2000 K and 30 $m{\cdot}s^{-1}$ from 2000 to 4000 K. The least-square linear fits also show very close values (see Fig. 13), including reported literature data [18]. Opposite to solid phase, these similarities are probably due to a small effect of a low solute content in the liquid (random structure).

As already mentioned for pure Pu [2], the most remarkable fact of these results is related to the *increase* of sound velocity with temperature. Such an observation is considered to be *anomalous* since most of materials present a negative temperature coefficient. A specific attention onto these atypical cases shows a correlation with a *volume contraction on their melting point* as for some semimetals (Bi, Sb, Ge, Si, Ga, Te), or even water. For all of these cases, the volume contraction is associated to a negative slope of the melting curve according to the Clausius–Clapeyron's law[2].

Concerning the f elements (*i.e.* lanthanides – 4f shell – and actinides – 5f shell -), two exceptions such as Ce [19,20] and Pu [2,18] are registered by presenting a volume contraction and then an increase of sound velocity occurring on melting and further up in the liquid state in a certain temperature range depending on the material. For these two cases the volume contraction is interpreted as an effect of the hybridization of their f electrons with the conduction bands [2,19,20]. For the specific case of Pu and its alloy, it would be due to the broadening and lowering of the 5f wave functions which consequently form overlapping energy bands with the 6d7s conduction shell. Then the body-centered cubic (bcc) structure ε phase existing prior to melting, for which the 5f electrons are rather localized, would be replaced by a lower symmetry (random structure) and a denser liquid phase where the participation in bonding of the so-called delocalized (or itinerant) 5f orbitals would be predominant.

The results on sound velocity measurements can be more easily understood and discussed in terms of compressibility, and more specifically of temperature coefficients. Indeed, both coefficients of sound velocity and adiabatic compressibility are related by the following expression:

$$\frac{1}{\chi_S}\left(\frac{d\chi_S}{dT}\right)_P = -\left(\frac{2}{c_L}\frac{dc_L}{dT} + \frac{1}{\rho}\frac{d\rho}{dT}\right), \tag{11}$$

by differentiating Eq. (7). In Eq. (11), since the second term is almost always negative (positive by including the sign of Eq. (11)) and due to its very low value (because of the high density of Pu), the $d\chi_S/dT$ sign *only depends* on the sign of dc_L/dT (more precisely on $-dc_L/dT$). In the general case for liquid metals, $dc_L/dT < 0$ (and thus $-dc_L/dT > 0$), and then $d\chi_S/dT > 0$: this corresponds to a loosening of structure with increasing temperature. In the particular case of pure and alloyed Pu, $d\chi_S/dT$ is then negative for $T_M < T < 2000$ and positive for $2000 < T < 4000$ K (see Fig. 13).

From these considerations, the hybridization of the f electrons with the conduction band associated with an increase of the atomic cohesion (and then decrease of the interatomic distance) due to their bonding, would lead to a decrease of compressibility ($d\chi_S/dT < 0$) and then to an increase of sound velocity ($dc/dT > 0$).

Moreover, it should be pointed out that most of the cited anomalous materials present a maximum of sound velocity (minimum of compressibility) as temperature increases, before exhibiting a negative temperature coefficient (normal behavior). For Pu, this phenomenon has been attributed to a competition of two opposing processes, *i.e.* the hybridization effect and the thermal motion that is probably predominant at high temperature [2]. Indeed, thermal motion induces an increase of the interatomic distance. The correlated increase of compressibility leads to a decrease of sound velocity. In that case, one would find again a normal behavior (with a negative temperature coefficient) of sound velocity. This tends to prove that thermal motion no longer allows delocalized f electrons to impose their character.

As reminded above, sound velocity measurements are very useful for providing equation of state (EOS) parameters calculations. Then, the isothermal bulk modulus B_T, the Grüneisen parameter Γ, and the specific heat ratio γ variations are presented in Figs 14–16, respectively for both pure Pu and δ-Pu 2.5 at.%. These data are reported here as a function of density ρ which is calculated from specific volume measurements since:

$$\rho = \rho_0 \frac{V_0}{V}, \tag{12}$$

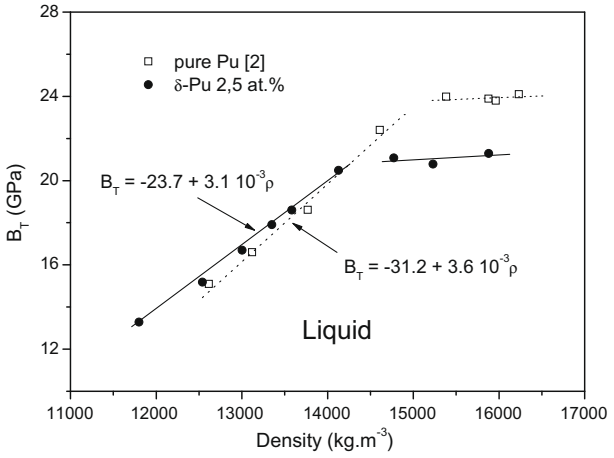

Fig. 14. Isothermal bulk modulus versus density of liquid δ-Pu 2.5 at.% and pure Pu [2].

[2] On melting, the dP/dT sign only depends on ΔV since ΔH and T (in K) are always positive.

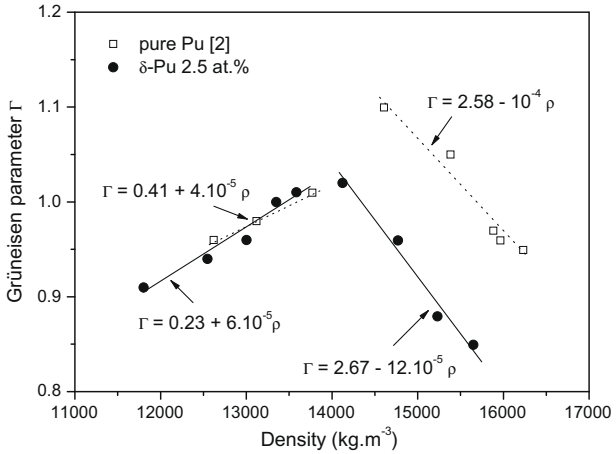

Fig. 15. Grüneisen parameter versus density of liquid δ-Pu 2.5 at.% and pure Pu [2].

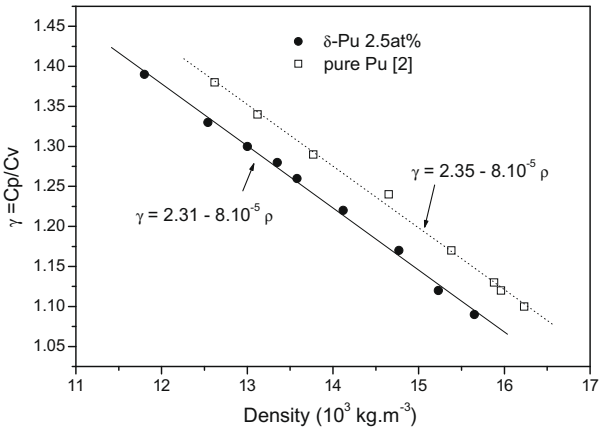

Fig. 16. Specific heats ratio γ versus temperature of liquid δ-Pu 2.5 at.% alloy and liquid pure Pu [2].

As for sound velocity, one can observe strong similarities between EOS parameters between pure and alloyed Pu.

Therefore, it is shown from Fig. 14 that the isothermal bulk modulus B_T is constant from the melting density down to around 15000 kg·m^{-3} and equals to 24 GPa and 21 GPa for pure Pu and δ-Pu 2.5 at.%, respectively. Then, it linearly decreases according to 3.6×10^{-3} GPa·kg^{-1}·m^3 and 3.1×10^{-3} GPa·kg^{-1}·m^3 coefficients with decreasing density (correlated to an increase of temperature). One observes that at low density (and then high temperature) values of both materials are very close, meaning the alloying effect is negligible in that density (temperature) range.

In Fig. 15, the Grüneisen parameter variation versus density presents a maximum at a density close to 15 000 kg·m^{-3} and 14 000 kg·m^{-3} for pure Pu and δ-Pu 2.5 at.%, respectively. The corresponding linear fits are $\Gamma = 2.58\text{–}10^{-4}\,\rho$ and $\Gamma = 2.67\text{–}12 \cdot 10^{-5}\,\rho$ for the high density range and $\Gamma = 0.41 + 4{\cdot}10^{-5}\,\rho$ and $\Gamma = 0.23 + 6 \cdot 10^{-5}\,\rho$ for the low density range. As for isothermal bulk modulus, very close values of both materials are found at low density.

The specific heats ratio $\gamma = C_p/C_v$ is also reported versus density in Fig. 16. γ linearly decreases with density (increases with temperature) according to $\gamma = 2.35\text{–}8 \cdot 10^{-5}\,\rho$ and $\gamma = 2.31\text{–}8 \cdot 10^{-5}\,\rho$ relations for pure Pu and δ-Pu 2.5 at.%, respectively. Then the alloy value is found to be a little bit smaller ($\sim 5.5 \cdot 10^{-2}$) than pure Pu one but its evolution with density is strictly the same.

It should be noticed that such a parameter does not surprisingly present any drastic change as for other previous ones. The reason should be explained from Eq. (9): by reminding that the expansion coefficient α is independent on temperature ($11{\cdot}10^{-5}$ K^{-1}), and Γ being of the order of unity, the second term $\alpha T\Gamma$ is small compared to one. Thus, it does not strongly influence the value of γ. Due to this argument, the observation of a maximum for Γ (ranging from 0.95 to 1.1: see Fig. 15) is not exhibited through the variation of γ for both pure alloyed Pu.

4. Conclusion

This paper is a review of the thermophysical properties of both the solid and liquid states of pure and alloyed Pu up to nearly 4000 K. We have focused our attention on the *liquid phase* which is here the main novelty of this article regarding the literature data, because of a very low number of papers dealing with this topic.

The effect of heating rate on pure (and alloyed) Pu using a pulse heating technique has been investigated. It has been shown the allotropic transition temperatures are systematically higher under rapid heating than the static measurements, but the needed deposited energy for reaching the liquid state, and consequently the melting point, is independent on the heating rate.

The heat transport properties of different plutonium alloys have been reported in the solid phase. A good agreement is obtained with reported literature data regarding heat capacity, thermal diffusivity and thermal conductivity measurements. It is shown that the deltagen elements composition has not a strong influence on these heat transport properties.

Sound velocity measurements of different solid plutonium alloys have been also investigated. They have confirmed an anomalous elastic softening of the δ phase. A specific behavior is obtained with the observation of an inflexion point for low deltagen contents that we correlate to the metastable region of the δ phase.

In addition to previous works on pure Pu, the thermophysical properties of liquid alloyed Pu have been investigated. Electrical resistivity, specific volume, heat capacity as for sound velocity and EOS parameters measurements are reported in this paper. As expected from earlier experiments on liquid pure Pu and due to the low deltagen elements content of the studied alloy, sound velocity (and consequently EOS parameters) of liquid alloyed Pu exhibits an odd behavior by presenting a maximum versus temperature (correlated to a minimum of compressibility). Such a phenomenon is interpreted by a competition between two opposing processes: delocalization of the 5f electrons and thermal motion which are the predominant effects at low and high temperature, respectively.

Acknowledgements

A special thank to A. Berthault for his huge contribution on pulse heating experiments. The author is indebted to his colleagues at CEA who contributed to the experimental works, specifically L. Arlès, C. Berthaut, M. Clément, F. Couvreur, D. Doytier, V. Eyraud, C. Roy and J.-M. Vermeulen.

References

[1] A. Berthault, L. Arlès, J. Matricon, Int. J. Thermophys. 7 (1986) 167.
[2] M. Boivineau, J. Nucl. Mater. 297 (1) (2001) 97.
[3] M. Boivineau, G. Pottlacher, Int. J. Mater. Prod. Technol. Special Issue: Challenges in Materials Properties Measurements 26(3/4) (2006) 217–246.
[4] S.S. Hecker, D.R. Harbur, T.G. Zocco, Prog. Mater. Sci. 49 (2004) 429.
[5] M. Boivineau, C. Cagran, D. Doytier, V. Eyraud, M.-H. Nadal, B. Wilthan, G. Pottlacher, Int. J. Thermophys. 27 (2) (2006) 507.
[6] C.E. Rollon, G.F. Gallegos, J. Therm. Anal. 21 (1981) 159.
[7] F.L. Oetting, R.O. Adams, J. Chem. Thermodyn. 15 (1983) 537.
[8] D.R. Stephens, J. Phys. Chem. Solids 24 (1963) 1197.

[9] J.R. Morgan, in: W.N. Miner (eds.), Proceedings of the of 4th International Conference on Plutonium and other Actinides, 1970, Warrendale, PA: The Metallurgical Society of AIME, 1970, pp. 669–678.
[10] F.H. Ellinger, C.C. Land, V.O. Struebing, J. Nucl. Mater. 12 (2) (1964) 226.
[11] R.O. Adams, F.L. Oetting, J. Nucl. Mater. 118 (1983) 269.
[12] J.F. Andrew, P.G. Klemens, in: 17th International Thermal Conductivity Conference, NBS, Gaithersburg, MD, USA, June 15–18, 1983, vol. 17, Plenum Publishing Corp., New York, NY (USA), 1983, pp. 209–218.
[13] O.L. Kruger, J.L. Robbins, in: 5th International Conference on Plutonium and Other-Actinides-1975, 1976, pp. 547–557.
[14] C.A. Calder, E.C. Draney, W.W. Wilcox, J. Nucl. Mater. 97 (1981) 126.
[15] A. Migliori, H. Ledbetter, A.C. Lawson, A.P. Ramirez, D.A. Miller, J.B. Betts, M. Ramos, J.C. Lashley, Phys. Rev. B 73 (5) (2006) 52101-1.
[16] A.C. Lawson et al., Philos. Mag. 86 (17–18) (2006) 2713.
[17] R.S. Hixson, M.A. Winkler, J.W. Shaner, Physica 139B (1–3) (1986) 893.
[18] M.D. Merz, J.H. Hammer, H.E. Kjarmo, J. Nucl. Mater. 51 (1974) 357.
[19] M. Boivineau, J.-B. Charbonnier, J.-M. Vermeulen, Th. Thévenin, High Press–High Temp. 25 (1993) 311.
[20] S.P. McAlister, E.D. Crozier, Solid State Commun. 40 (1981) 375.